Magnetism of Less Common Cobalt-Rich Alloys

B. DAS,[1,2] B. BALAMURUGAN,[1,2] W.Y. ZHANG,[1,2)] R. SKOMSKI,[1,2] E.S. KRAGE,[2,3] S.R. VALLOPPILLY,[2] J.E. SHIELD,[1,4], and D.J. SELLMYER [1,2]

[1] Nebraska Center for Materials and Nanoscience, University of Nebraska, Lincoln, NE-68588, USA

[2] Department of Physics and Astronomy, University of Nebraska, Lincoln, NE-68588, USA

[3] Department of Physics, South Dakota University, Brookings, SD-57007, USA

[4] Department of Mechanical and Materials Engineering, University of Nebraska, Lincoln, NE-68588, USA

Abstract—Alternative permanent-magnet materials with intermediate performance, such as $K_1 \geq 1$ MJ/m^3, are investigated experimentally. Our focus is on the structural and magnetic properties of bulk $YCo_{5-x}Fe_x$ and on rare-earth-free transition-metal alloys such as TM_xCo_{100-x} (TM = Zr, Hf). $YCo_{5-x}Fe_x$ alloys (x = 0 to 0.75), which crystallize in the hexagonal $CaCu_5$-type structure, exhibit an improved of anisotropy and magnetization as x increases from 0 to 0.75, but the anisotropy increase is much less pronounced than recent theoretical predictions. Zr_xCo_{100-x} and Hf_xCo_{100-x} exhibit reasonable room-temperature hard-magnetic properties, such as coercivities of 0.10 to 0.28 T and magnetizations of 0.60 to 0.94 T.

I. INTRODUCTION

Rare-earth cobalt alloys, especially $SmCo_5$ and Sm_2Co_{17}, are the first rare-earth permanent magnets and continue to be useful for high-temperature applications [1-2]. In particular, RCo_5 (R = Sm, Y), which crystallizes in the hexagonal $CaCu_5$-type structure, exhibit high anisotropies at room temperature and above, and there are continuing theoretical [3-6] and experimental [7, 8] attempts to further improve their magnetic properties by doping with a third element, such as B and Fe. For example, recent density-functional calculations have shown that Fe in $RCo_{5-x}Fe_x$ increases both the magnetic anisotropy constant K_1 and magnetic polarization J_s for small fractions of Fe (x ≤ 0.35) [4]. However, it is unclear to what extent these predictions are consistent with experiment.

Beyond the hexagonal 1:5 and rhombohedral or hexagonal 2:17 structures, there are other noncubic Co-rich intermetallics, and atomic substitutions yield a rich variety of related pseudoternary compounds. For example, Zr_2Co_{11} and $HfCo_7$ are part of the ongoing search for alternative permanent-magnet alloys due to their high Curie temperatures (T_c > 600 K), and non-cubic structures, which can create high anisotropy in these materials [9-12]. The crystal structure of the last alloy is only partially known, but unrelated to the hexagonal $SmCo_5$ and $SmCo_7$. Our current research focuses on the improvement of magnetic properties by further doping or alloying Y alloys with a third element such as Fe and search for rare-earth-free alloys with high $K_1 \geq 1$ MJ/m^3.

II. EXPERIMENTAL METHODS

$YCo_{5-x}Fe_x$ alloys with different Fe concentrations (x = 0, 0.25, 0.50, and 0.75) were prepared using a conventional arc-melting technique followed by high-temperature thermal annealing at 1100 °C for 48 hrs . The alloys were then ground into small particles for structural and magnetic investigation. To determine K_1, the as-produced $YCo_{5-x}Fe_x$ particles were embedded in an epoxy resin and the easy axes were subsequently aligned with a magnetic pulse field of 12 T.

The Zr_xCo_{100-x} and Hf_xCo_{100-x} alloys were produced by melt spinning. For this, high-purity elements with appropriate compositions were mixed homogeneously using conventional arc melting and subsequently melt spun to obtain ribbons. The rapid cooling during the melt spinning process is advantageous for controlling phase purity and microstructure, which is important to realize the permanent-magnet properties of the alloys.

X-ray diffraction (XRD: Rigaku D/Max-B diffractometer), transmission-electron microscopy (TEM: JEOL 2010 with an acceleration voltage of 200 kV), energy dispersive x-ray analysis (EDX, JEOL JSM 840A scanning electron microscope), and SQUID magnetometry were used for characterization.

Corresponding author : B. BALAMURUGAN
(e-mail : bbalasubramanian2@unl.edu)

III. STRUCTURAL AND MAGNETIC PROPERTIES OF $YCo_{1-x}Fe_x$ BULK ALLOYS

The structural properties of as-produced $YCo_{5-x}Fe_x$ alloys as a function of Fe concentration were investigated using x-ray diffraction. For example, Fig. 1(a) shows the XRD patterns for $YCo_{5-x}Fe_x$ ($0 \le x \le 0.75$).

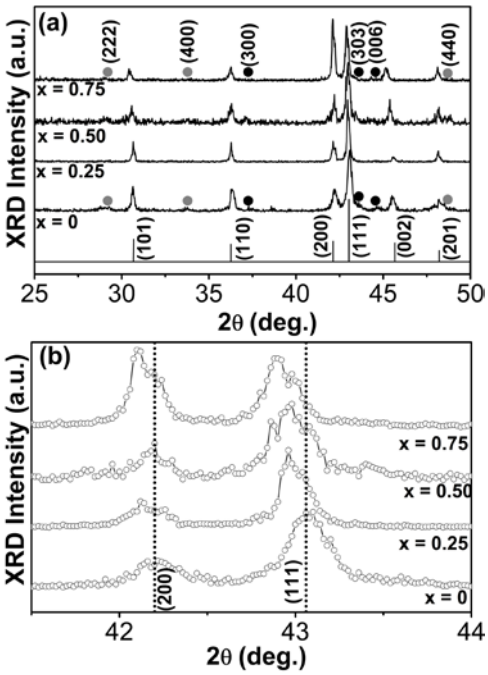

Fig. 1 X-ray diffraction patterns: (a) $YCo_{5-x}Fe_x$ alloys of different Fe concentrations with the standard positions and relative intensities of the diffraction peaks corresponding to YCo_5 (vertical lines), Y_2Co_{17} (black dots) and Y_2O_3 (gray dots), and (b) the expanded x-ray diffraction patterns at $2\theta = 41.5°$ to $44.0°$, showing the composition-dependent shift in the peak positions as guided by the dotted lines.

The standard peak positions and relative intensities of the diffraction peaks corresponding to the hexagonal $CaCu_5$-type structure of YCo_5 are shown as black solid vertical lines [13]. The XRD peaks are sharp and intense, revealing well-developed polycrystallites, and also in good agreement with the hexagonal $CaCu_5$-type structure. A minor presence of Y_2O_3 and Y_2Co_{17} is, however, evident from the weak diffraction peaks corresponding to these phases, as indicated by the respective gray and black dots in Fig. 1(a) [14, 15].

The weak diffraction peaks corresponding to Y_2O_3 phase, such as (222) and (440) in Fig. 1(a), are also broad due to the well-known crystallite size of Y_2O_3. In addition, the standard-maximum intensity (330) peak of Y_2Co_{17} phase also appears as a weak hump near to most intense (111) peak of the YCo_5 phase. Note that conventional preparation techniques (such as arc melting followed by high-temperature thermal annealing for bulk RCo_5 alloys) are generally expected to produce a small fraction of 2:17 phase during the cooling process [16, 17].

We also have carried out Rietveld analysis to quantify these phases [18], but an accurate refinement was limited by the broadness of Y_2O_3 peaks and a shift in the peak positions of YCo_5 phase along with an increased intensity of the (200) peak on substituting Fe for Co in $YCo_{5-x}Fe_x$. Nevertheless, as an example, Rietveld analysis for $YCo_{4.75}Fe0.25$ typically yields 95.1 wt. % of $YCo_{4.75}Fe_{0.25}$, 0.6 wt. % of Y_2O_3 and 4.3 wt. % of Y_2Co_{17}.

To trace the changes in the YCo_5 lattice upon Fe substitution, we have expanded the XRD patterns of the as-produced $YCo_{5-x}Fe_x$ alloys in the 2θ range from 41.5° to 44.0°, as shown in Fig. 1(b). We see a systematic shift in the angular positions of the Braggs reflections from YCo_5 phase towards lower angles as x increases from 0 to 0.5. This corresponds to a lattice expansion upon the substitution of Fe for Co. For example, the lattice constants increased from $a = 4.940$ Å and $c = 3.981$ Å to $a = 4.950$ Å and $c = 4.009$ Å on varying x from 0 to 0.75. In addition, the intensity of (200) peak also increases as compared to that of (111) peak as x increases from 0 to 0.75. This indicates the stabilization of the hexagonal $CaCu_5$-type structure in $YCo_{5-x}Fe_x$ alloys for x up to 0.75.

In order to determine the anisotropy constant K_1, we have measured the parallel and perpendicular *M-H* curves at 300 K for magnetically aligned $YCo_{5-x}Fe_x$ alloys, as shown for YCo_5 , Fig. 2(a), and $YCo_{4.5}Fe_{0.5}$, Fig. 2(b).

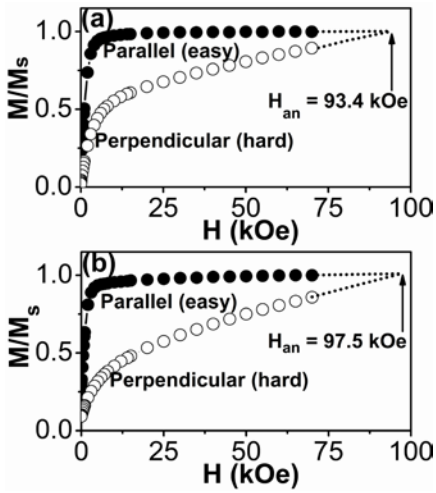

Fig.2 Parallel and perpendicular *M-H* curves measured at 300 K : (a) aligned YCo_5 and (b) aligned $YCo_{4.5}Fe_{0.5}$.

Corresponding author : B. BALAMURUGAN
(e-mail : bbalasubramanian2@unl.edu)

The straight approach of the perpendicular curves to the saturation indicates that the effect of K_2 is very small. In addition, a striking feature of these curves is that the perpendicular *M-H* intersects the magnetization axis at $M > 0$. This feature can be presumably due to the collective effects of the grain-misalignment and weak presence of secondary phases..

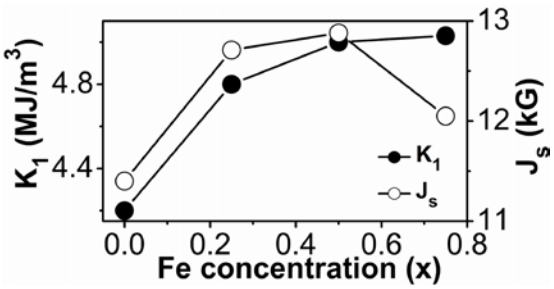

Fig. 3 Room-temperature magnetic anisotropic constant K_1 and saturation magnetic polarization J_s of $YCo_{5-x}Fe_x$ as a function of Fe concentration (x).

The K_1 of the hard YCo_5 phase can be, however, obtained from the magnetic anisotropic field H_{an}. As indicated in Fig. 2, H_a is given by the intercept between the parallel and linear portion of the perpendicular curves, and this method has an error of typically less than 10% [1, 19, 20]. Figure 3 shows the corresponding values of K_1 and J_s of $YCo_{5-x}Fe_x$ as a function of Fe concentration.

As x varies from 0 to 0.75, the room-temperature anisotropy of $YCo_{5-x}Fe_x$ improves from 4.2 to 5.0 MJ/m^3, and the magnetization also increases. This is consistent with previous findings, including theoretical calculations [4-7]. Furthermore, the moderate improvements due to Fe substitutions in rare-earth cobalt magnets have long been explored and exploited in industry. Even in cases where Fe leaves the magnetic properties of a rare-earth cobalt alloy unchanged, Fe substitution is preferred, because Fe is much cheaper than Co.

Interestingly, density-functional calculations tend to overestimate the anisotropy difference between YCo_5 and $YCo_{5-x}Fe_x$. For example, they predict that K_1 increases from 2.7 MJ/m^3 in YCo_5 to 4.7 MJ/m^3 in $YCo_{4.65}Fe_{0.35}$ [4]. Similarly, the calculated band-filling dependence of the magnetic anisotropies also reveals an increase in K_1 from about 8.3 MJ/m^3 (YCo_5) to a maximum of 26.5 MJ/m^3 for YCo_4Fe [7]. These theoretical calculations were performed at zero temperature, but the temperature dependence of the anisotropy of YCo_5 is notoriously weak [2] and cannot account for the high anisotropy values predicted by some of the calculations.

IV. RARE-EARTH-FREE Zr_xCo_{100-x} and Hf_xCo_{100-x} BULK ALLOYS

The XRD patterns and TEM images of Zr_xCo_{100-x} ($16 \le x \le 21$) show the presence of predominant Zr_2Co_{11} phase having a rhombohedral structure, along with comparatively weak hcp Co and cubic Zr_6Co_{23} phases [21, 22]. The soft magnetic Co and Zr_6Co_{23} phases are expected to form exchange coupling to the hard magnetic Zr_2Co_{11} phase.

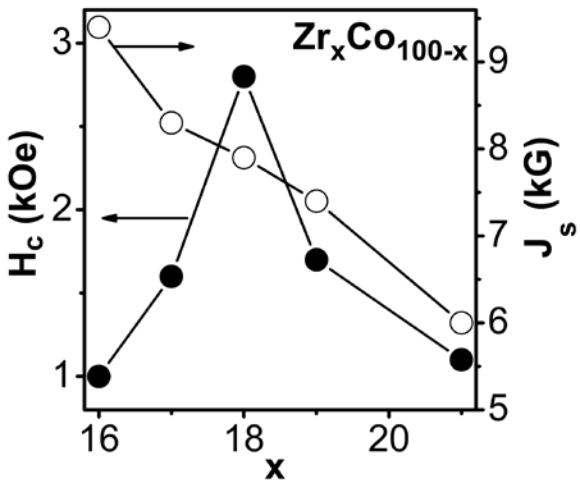

Fig. 4 Coercivity H_c and saturation polarization J_s measured at 300 K for Zr_xCo_{100-x} alloys as a function of Zr concentration x.

Figure 4 shows that Zr_xCo_{100-x} is hard-magnetic, with coercivities larger than 1 kOe and appreciable magnetizations between 0.60 and 0.95 T at room temperature. The coercivity changes in Fig. 4 mainly depend on the amount of hard magnetic Zr_2Co_{11} phase in these samples [22].

Similarly, H_c increases from 0.05 to 1.8 kOe at 300 K on increasing x from 0 to 12.5 in Hf_xCo_{100-x} [23]. For x = 12.5, Hf_xCo_{100-x} forms a $HfCo_7$ phase having orthorhombic structure. Available literature data on the unit cells are contradictory and however, a careful analysis of the question goes far beyond the present paper and will be discussed elsewhere.

It is worthwhile mentioning that *M-H* curves of both Zr-Co and Hf-Co do not saturate even in fields of 7 T. While the approach to saturation is relatively slow for isotropic magnets, this nevertheless confirms the high

Corresponding author : B. BALAMURUGAN
(e-mail : bbalasubramanian2@unl.edu)

magnetic anisotropy of the materials. More explicitly, K_1 was evaluated from the high-field magnetization curves of these alloys (H ≥ 30 kOe) using the law of approach to saturation method [24]. The corresponding room-temperature anisotropy values are 1.1 and 1.6 MJ/m^3 for $Zr_{18}Co_{82}$ and $Hf_{12.5}Co_{87.5}$, respectively.

V. CONCLUSIONS

The structural and magnetic properties of $YCo_{5-x}Fe_x$ and rare-earth-free transition metal alloys such as Zr_xCo_{100-x} and Zr_xCo_{100-x} were investigated. The magnetic anisotropy constant K_1 improves from 4.2 to 5.0 MJ/m^3 at 300 K along with an improvement of J_s on varying x from 0 to 0.75 in $YCo_{5-x}Fe_x$. This general trend is consistent with recently reported theoretical investigations based on density-functional and band-filling calculations. However, it seems that density-functional calculations significantly overestimate the anisotropy enhancement due to Fe, and further research will be necessary to explain the discrepancies.

Zr-Co and Hf-Co alloys also exhibit a fairly high anisotropy of $K_1 \geq 1.0$ MJ/m^3. Concerning price and performance, these rare-earth-free permanent-magnet materials are generally intermediate between Ba ferrite and rare-earth permanent magnets, and future research will show whether any of these materials can be developed into industrial magnets.

ACKNOWLEDGMENT

This work is supported by US DOE (DE-FG02-04ER46152, DJS), ARPA-E (DE-AR 0000046, B.B. and B.D.), NSF-MRSEC (Grant No. DMR-0820521, R.S. and J.E.S.), BREM (WYZ), and NCMN.

REFERENCES

[1] K. Strnat, G. Hoffer, J. Olson, W. Ostertag, and J.J. Becker, *J. Appl. Phys.* 38, 1001 (1967).
[2] R. Skomski and J.M.D. Coey, *Permanent Magnetism*, Institute of Physics, Bristol 1999.
[3] P. Larson, I. I. Mazin, and D. A. Papaconstantopoulos, *Phys. Rev. B* 69, 134408 (2004).
[4] I. Opahle, M. Richter, M.D. Kuz'min, U. Nitzsche, K. Koepernik, L. Schramm, *J. Magn. Magn. Mater.* 290-291, 374 (2005).
[5] G.H.O. Daalderop, P.J. Kelly, and M.F.H. Schuurmans, *Phys. Rev. B* 53, 14415 (1996).
[6] L. Steinbeck, M. Richter, and H. Eschrig, *Phys. Rev. B* 63, 184431 (2001).
[7] H. Ido, K. Konno, H. Ogata, K. Sugiyama, H. Hachino, M. Date, and K. Maki, *J. Appl. Phys.* 70, 6128 (1991).
[8] J.J.M. Franze, N.P. Thuy, and N.M. Hong, *J. Magn. Magn. Mater.* 72, 361 (1988).
[9] A.M. Ghemawat, M. Foldeaki, R.A. Dunlap, and R.C. O' Handley, *IEEE Trans. Mag.* 25, 3312 (1989).
[10] G.V. Ivanova, N.N. Schegoleva, and A.M. Gabay, *J. Alloys. Comp.* 423, 135 (2007).
[11] K.H.J. Buschow, J.H. Wernick. And G.Y. Chin, *Journal of the Less Common Metals*. 59, 61 (1978)..
[12] K.H.J. Buschow, *J. Appl. Phys.* 53, 7713 (1982).
[13] *ICDD-International Centre for Diffraction Data*, Card No. 01-071-7515.
[14] *ICDD-International Centre for Diffraction Data*, Card No. 04-043-1036.
[15] *ICDD-International Centre for Diffraction Data*, Card No. 04-005-4950.
[16] J.T.E. Galindo, J.A. Matutes-Aquino, M. Costes, and J.M. Broto, *J. Appl. Phys*. 105, 07A725 (2009).
[17] J.T.E. Galindo, F.J. Rivera Gomez, and J.A. Matutes-Aquino, *J. Appl. Phys.* 99, 08B512 (2006).
[18] H.M. Rietveld, *J. Appl. Cryst*. 2, 65 (1969).
[19] Y.Q. Guo, W. Li, J. Luo, W.C. Feng, and J.K. Liang, *J. Magn. Magn. Mater.* 303, e367 (2006).
[20] Y. Guo, W. Feng, W. Li, J. Luo, and J. Liang, *J. Appl. Phys.* 101, 023919 (2007).
[21] W.Y. Zhang, S. Valloppilly, X.Z. Li, R. Skomski, J.E. Shield, and D.J. Sellmyer, *IEEE Trans. Mag.* (in press).
[22] W.Y. Zhang, X.Z. Li, S. Valloppilly, R. Skomski, J.E. Shield, and D.J. Sellmyer (in preparation).
[23] B. Das, B. Balamurugan, V.R. Shah, R. Skomski, and D.J. Sellmyer (in preparation).
[24] G.C. Hadjipanayis, D.J. Sellmyer, and B. Brandt, *Phys. Rev. B* 23, 3349, 1978.

Corresponding author : B. BALAMURUGAN
(e-mail : bbalasubramanian2@unl.edu)